



Potential CO₂ removal from enhanced weathering by ecosystem responses to powdered rock

Daniel S. Goll^{1,2}✉, Philippe Ciais², Thorben Amann³, Wolfgang Buermann¹, Jinfeng Chang⁴, Sibel Eker⁵, Jens Hartmann³, Ivan Janssens⁶, Wei Li⁷, Michael Obersteiner⁸, Josep Penuelas^{9,10}, Katsumasa Tanaka^{2,11} and Sara Vicca⁶

Negative emission technologies underpin socioeconomic scenarios consistent with the Paris Agreement. Afforestation and bioenergy coupled with carbon dioxide (CO₂) capture and storage are the main land negative emission technologies proposed, but the range of nature-based solutions is wider. Here we explore soil amendment with powdered basalt in natural ecosystems. Basalt is an abundant rock resource, which reacts with CO₂ and removes it from the atmosphere. Besides, basalt improves soil fertility and thereby potentially enhances ecosystem carbon storage, rendering a global CO₂ removal of basalt substantially larger than previously suggested. As this is a fully developed technology that can be co-deployed in existing land systems, it is suited for rapid upscaling. Achieving sufficiently high net CO₂ removal will require upscaling of basalt mining, deploying systems in remote areas with a low carbon footprint and using energy from low-carbon sources. We argue that basalt soil amendment should be considered a prominent option when assessing land management options for mitigating climate change, but yet unknown side-effects, as well as limited data on field-scale deployment, need to be addressed first.

Rapid and massive deployment of negative emission technology (NET) to remove carbon from the atmosphere is needed if we are to achieve the climate stabilization targets agreed at the 2015 Paris Agreement¹. A range of nature-based NETs have been proposed that offer the advantage of low technological barriers and modest energy demands. However, their potential and scalability² are uncertain and some compete with other land uses for land, water and nutrients^{3,4}.

Nature-based land NETs rely on biomass carbon sequestration through interventions such as planting forests, sustainable forestry, soil carbon sequestration from increased inputs to agricultural soils and biochar additions, and the enhancement of weathering. Enhanced weathering offers the advantage that it can be deployed with other land uses. Yet, there are few studies about this NET^{3–6}, and to our knowledge, regional and global scalability were investigated only for arable land⁷, with co-benefits for biomass and soil carbon sequestration remaining largely omitted. Here we focus on one specific and promising application—the amendment of soils with basalt dust (BD). This choice is justified by the vast availability of basalt⁸, its high weatherability⁹ and co-benefits^{5,10}.

Basalt soil amendment

Soil amendment is the addition of any material to a soil to enhance its functioning or, in other words, its suitability for a given use. Here we consider the enhanced weathering from BD to accelerate the reaction of atmospheric CO₂ with the silicates contained in basalt¹¹. The silicate grains chemically react with CO₂ to form bicarbonate dissolved ions; these are transported by rivers to the oceans

and potentially stored for hundreds of years and longer, depending on calcium carbonate sedimentation processes¹². In addition to this abiotic CO₂ removal (CDR) pathway, amending soils with BD enhances soil fertility by releasing nutrients, buffering low soil pH and stabilizing soil organic matter¹³, and can improve soil water retention¹⁴, thereby promoting plant growth and CDR in agriculture^{15–17} and forestry¹⁰. This biotic CDR pathway for enhanced weathering^{18,19} has so far been omitted in assessments of the climate mitigation potential of this NET^{6,20}.

BD has mainly been considered for application in agriculture^{5,7,21}, less so in forestry²², and occasionally in natural ecosystems and ecosystems under restoration⁶. Yet, biomass production and carbon storage in a wide range of unmanaged systems^{23–26} is limited by essential nutrients, such as phosphorus (P) or potassium (K), which are contained in basalt. In several regions the positive effect of elevated CO₂ on biomass production hinges on the availability of P²⁷. Thus, BD amendment could deliver additional P to sustain or even increase biomass production, and subsequent CDR, not only in managed but also in natural systems.

CDR potential

To illustrate and explore the full CDR potential from BD application for present-day conditions, we used a land surface model (ORCHIDEE-CNP) that resolves weathering processes and how the release of P stimulates ecosystem carbon sequestration. This model includes a simplified weathering module calibrated against data available from short-term studies, in view of the scarcity of long-term field-scale experiments^{21,28,29}. We used an idealized

¹Institute of Geography, University of Augsburg, Augsburg, Germany. ²Laboratoire des Sciences du Climat et de l'Environnement, CEA-CNRS-UVSQ-Université Paris-Saclay, Gif-sur-Yvette, France. ³Institute for Geology, Center for Earth System Research and Sustainability, University Hamburg, Hamburg, Germany.

⁴College of Environmental and Resource Sciences, Zhejiang University, Hangzhou, China. ⁵International Institute for Applied Systems Analysis, Laxenburg, Austria. ⁶Plants and Ecosystems (PLECO), University of Antwerp, Antwerp, Belgium. ⁷Ministry of Education Key Laboratory for Earth System Modeling, Department of Earth System Science, Tsinghua University, Beijing, China. ⁸Environmental Change Institute, University of Oxford, Oxford, UK. ⁹CREAF, Bellaterra, Spain. ¹⁰CSIC, Global Ecology Unit CREAF-CSIC-UAB, Bellaterra, Spain. ¹¹Earth System Risk Analysis Section, Earth System Division, National Institute for Environmental Studies (NIES), Tsukuba, Japan. ✉e-mail: dsgoll123@gmail.com

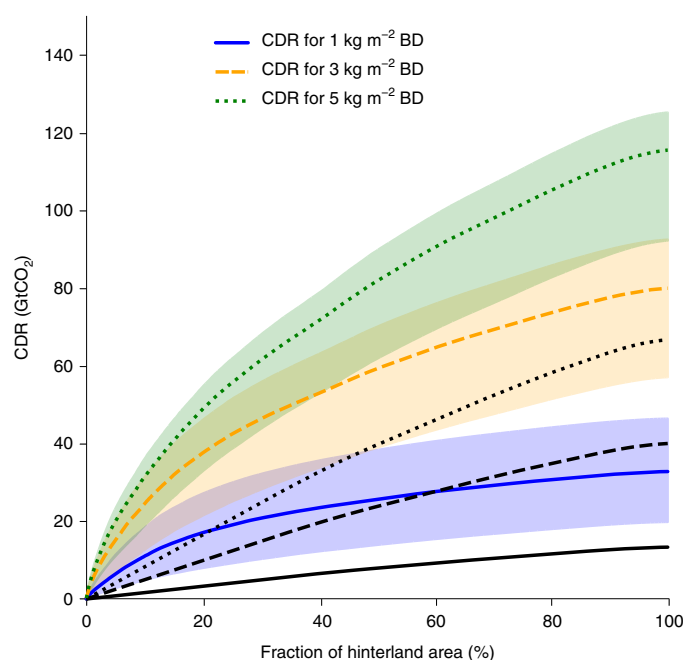


Fig. 1 | CDR over the five decades after a one-time application of BD to global hinterland. Total CDR (colour), as well as abiotic CDR alone (black), are shown for three application scenarios: 1, 3 and 5 kg m⁻² of BD. The range of CDR per scenario (shaded area) illustrates the uncertainty in P release from basalt.

scenario in which a single BD dose was applied to global vegetated hinterland (that is, travel distance of >3 h from the next small city or town³⁰; Supplementary Fig. 1) where the likelihood of interference with human activities is low (less than 1% of the global population lives in hinterlands)³⁰. It is not intended to reflect a realistic deployment scenario, but was chosen to identify sparsely populated regions with high CDR potential. We also performed a baseline simulation without BD application. We analysed the average biotic and abiotic CDR over five decades after a one-time BD application. A particle size was chosen such that it dissolves within five decades after application under most conditions (Extended Data Fig. 1). See Methods for a description of the model, the experimental design and details of the analysis.

We found that the application of 5 kg m⁻² of BD over a hinterland area of 55 million km² results in a CDR potential of 2.5 GtCO₂ yr⁻¹ over 50 years. This is higher than an earlier estimate for croplands of ~2 GtCO₂ yr⁻¹ (ref.²¹) for a comparable amount of BD (~6 Gt) but a much smaller area (~8 million km²), which did not account for biotic responses. The biotic pathway contributes about half (40–58%) of global CDR (Fig. 1). With increasing BD application, less CO₂ is removed per amount of BD added (Extended Data Figs. 1 and 2 and Supplementary Fig. 2), which suggests a general limit to the extent that CDR can be augmented by adding larger amounts of basalt to soils. Regionally, we find that the biotic pathway contribution to CDR is highly variable (32–80%; that is, 25th–75th percentile of data lumped from all 9 BD experiments; Fig. 2b) and is more influenced by ecosystem type than application rate, basalt P content (Supplementary Figs. 3 and 4) or climate zone. The strongest biotic CDR occurs in tropical regions on P-depleted soils where the addition of P in basalt enhances wood production and biomass carbon storage (Supplementary Note 1.2 and Supplementary Fig. 6). In Siberia, a high biotic CDR is predicted in regions where P released from BD enhances background P inputs by several orders of magnitude (Supplementary Fig. 5). The few available mineral P fertilizer experiments indicate positive biomass responses in boreal systems²⁵.

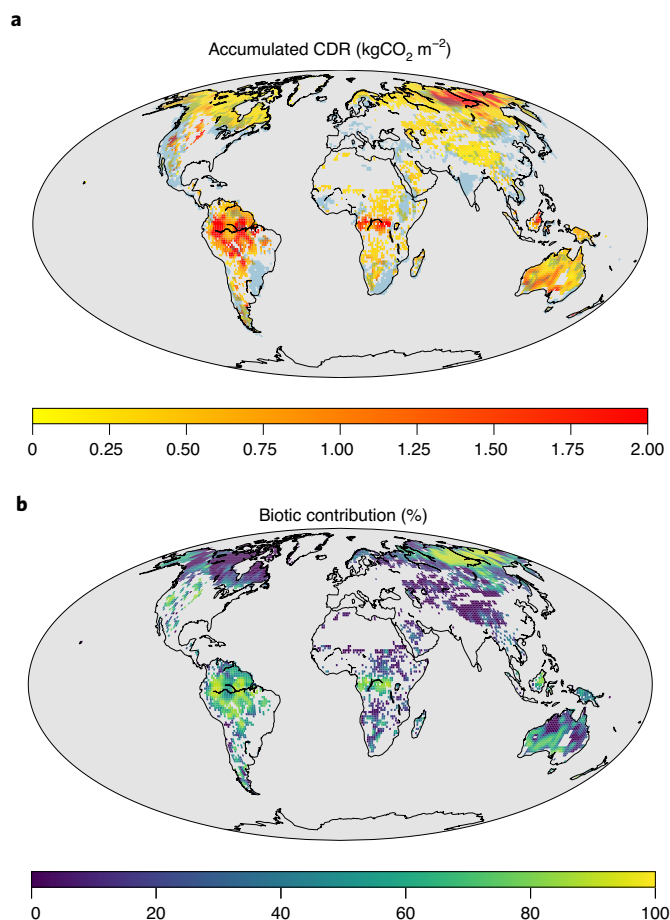


Fig. 2 | Spatial pattern of total CDR, and the biotic contribution, of BD application to global hinterland. a, b, CDR over the five decades after a one-time application of BD of 1 kg m⁻² (simulation A2) (a), and the fraction contributed by the biotic pathway (b). The blue dots in a show locations of near-surface basalt reserves from ref.⁵⁰.

Limitations and concerns

A major limitation to achieving the full CDR potential is the economic cost of mining, crushing and grinding basalt, and applying BD on targeted areas²¹. Under the conservative assumption of no technological innovation, we derived a supply cost curve for CDR by BD applied by helicopters or fixed-wing aircraft equipped with agricultural spreaders^{31–34} that are used to spread basalt in the form of free-flowing dust³⁴ or slurry³³ and have low requirements for ground infrastructure. Modified large aerial tankers such as those currently used for firefighting have >10 times the range and carrying capacities of small aircraft and could provide means to spray dust on large areas. We also assume that there are no bottlenecks on the supply side of basalt. We estimated that a global average of 0.2 GtCO₂ yr⁻¹ could be removed over a period of 50 years for regional costs lower than US\$100 per tCO₂ and up to 2.5 GtCO₂ yr⁻¹ in a more costly scenario for ~US\$500 per tCO₂ (Table 1, Fig. 3). The average costs are generally higher than estimates for BD deployment in agriculture and in coastal zones ranging between US\$50–200 per tCO₂ (refs.^{7,20,21}), owing to higher application costs. Modes of application other than by aircraft could help to reduce costs greatly, although substantial investment in the development of technologies such as airships and drones or alternatives such as railways and pipelines would be needed. If only abiotic CDR is considered as in previous assessments, the costs would exceed US\$550 per tCO₂ (Fig. 3).

Table 1 | Global CDR of BD for regional costs lower than US\$50, 100, 250, 500 and 1,000 per tCO₂ during the five decades after a one-time application of BD to global hinterland

Regional costs	Global average costs	Global CDR	Basalt required	Area required
<US\$100 per tCO ₂	US\$79 per tCO ₂	0.2 GtCO ₂ yr ⁻¹	0.2 Gt yr ⁻¹	2 × 10 ⁶ km ²
<US\$250 per tCO ₂	US\$156 per tCO ₂	0.8 GtCO ₂ yr ⁻¹	0.6 Gt yr ⁻¹	10 × 10 ⁶ km ²
<US\$500 per tCO ₂	US\$331 per tCO ₂	1.7 GtCO ₂ yr ⁻¹	2.5 Gt yr ⁻¹	25 × 10 ⁶ km ²
<US\$1,000 per tCO ₂	US\$513 per tCO ₂	2.5 GtCO ₂ yr ⁻¹	5.5 Gt yr ⁻¹	55 × 10 ⁶ km ²

Results of total CDR are shown from the most cost-efficient application scenario. In addition, global average CDR costs as well as the required land area and the amount of BD are given.

Thus, the additional carbon sequestration in ecosystems from the release of P is critical to make this technology competitive.

The second limitation is the extra greenhouse gas (GHG) emissions associated with the mining, crushing and grinding of rocks, and their distribution, which will partly offset the CDR benefits^{7,35}. On the basis of a compilation of present-day GHG emissions³⁶ for freight transport and energy generation (see Methods), we found that such emissions depend on the mode and distance of transportation, as well as on the energy production system in the NET technological chain. In contrast to cropland application^{7,21}, the spreading and transport of basalt are the dominant source of GHG emissions even if coal is used for energy generation (Extended Data Figs. 3 and 4). If BD were to be applied using aircraft, the GHG emissions from air transport would offset the median CDR benefits (280 kgCO₂ per tonne of basalt) for distances >450 km from airports (Extended Data Fig. 3 and Supplementary Fig. 8), but regionally substantial net negative emission could still be achieved even for remote (>1,000 km) regions where CDR potential is high (for example, Amazonia and Siberia; Fig. 2a and Supplementary Fig. 2). GHG emissions from transport and deployment of basalt depend on distance and transport technology (0.5–62 kgCO₂e per tonne of basalt per 100 km). The emissions from the energy mix used for producing BD as well as emissions from building infrastructure (0.6–46 kgCO₂e per tonne of basalt) are of secondary importance unless target sites are close to mines (Extended Data Fig. 4). Note that these are conservative estimates, as GHG emissions can be expected to decrease over time owing to innovation and progress in renewable energy transition.

A source of concern is the environmental impact of massive BD deployment in natural systems: although positive impacts have been suggested^{7,14}, the effects of BD application on eutrophication of aquatic systems, on biodiversity, on biosphere–atmosphere feedbacks, and on air, water and soil pollution still require thorough assessment. Moreover, application of fine (<10 µm) particles may also pose health risks³¹. Depending on how and where BD is deployed, negative side-effects could include albedo changes, damage to plant and wildlife tissue, and BD losses from wind transport³⁷. Therefore, pre-treatment of BD (for example, pellets, coatings or suspensions)^{29,33,34} and use of repeated application of smaller doses should be explored to reduce some of the potential negative side-effects. While soil pollution can be avoided by choosing basalt with low pollutant content or pre-treatment²⁹, risks related to affecting river chemistry and biodiversity do not depend only on the dose of BD, but also on the ecosystem status and on the fate of the P released from BD. On the basis of our exploratory modelling, we find low risks for negative effects of P leaching on water quality for most

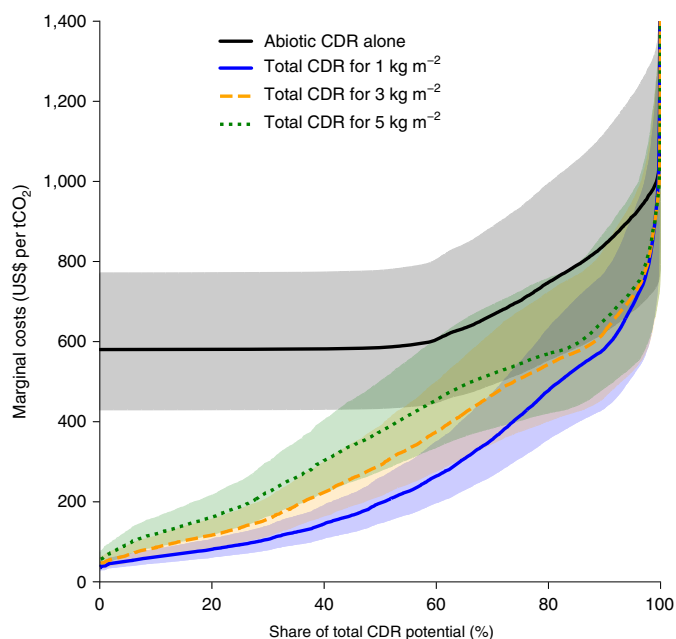


Fig. 3 | Cost of CDR over the five decades after a one-time application of BD to global hinterland. Data points (that is, model pixels) were ranked according to their marginal costs (from low to high). The horizontal axis shows the respective accumulated share of the global CDR potential. Three application scenarios are shown: 1, 3 and 5 kg m⁻² of BD for total CDR (colour), as well as for abiotic CDR alone (black). Cost uncertainty (shaded areas) illustrates uncertainty in costs for mining, crushing, grinding and airborne application.

aquatic systems for addition of ≤5 kg m⁻² of basalt (Supplementary Note 3 and Extended Data Figs. 5 and 6), but field-scale experiments are needed to validate our findings. Potential positive side-effects are alleviating deficiency of plant nutrition, and reducing nitrous oxide emissions and nitrogen leaching⁵, in regions affected by the extinction of wildlife³⁸ and high anthropogenic nitrogen deposition^{39,40}. The impact on terrestrial biodiversity is difficult to assess owing to scarce data. In general, positive relationships between bacteria, invertebrate and tree diversity and soil P or K content are reported for a wide range of ecosystems^{41,42}, while negative impacts have been shown for grassland communities⁴³. Targeted field-scale experiments are needed to assess the response of biodiversity to rock powder additions and associated inputs of plant nutrients.

Scalability and barriers

BD amendment was here reappraised as a promising NET that could be leveraged to help reach ambitious climate targets, given its previously overlooked enhancement of biological carbon sequestration. Several aspects of this technology advocate for rapid upscaling. First, it can be co-deployed, minimizing interference with other land uses. Second, there are clear co-benefits for other land uses such as crop and fibre production^{5,14–17}, the revitalization of the natural P pump⁴⁴, the alleviation of anthropogenic stoichiometric imbalances⁴⁰ and soil degradation⁴⁵. These provide incentives for BD application in managed and natural ecosystems. Third, extracting basalt and applying BD at a large scale would provide a new market for the mining industry currently suffering overcapacity and the accumulating overburden material¹⁸. Basalt mining could also replace jobs in the declining coal mining sector, facilitating just transitions towards renewable energy⁴⁶. Last, a mix of basalt and waste products such as phosphate gypsum and alkaline industrial waste (for example, steel slag or concrete from demolition⁷) could be used—following the idea of the inevitability of a transition towards a regenerative

circular economy (as acknowledged by China, Japan, Canada and the European Union⁴⁷). Our findings show that to sustain a global CDR of 1.3 GtCO₂yr⁻¹, a minimum amount of 1.1 Gt yr⁻¹ of basalt is sufficient (Table 1) if applied to regions with the largest CDR potential (not accounting for carbon emissions from production and deployment of BD). This indicates the possibility of a higher CDR per unit mass of basalt than for cropland application⁷.

Several societal, political, environmental and technological barriers would need to be overcome before a widespread deployment of BD amendments could be implemented. First, criteria for the selection of deployment sites and monitoring of CDR for carbon crediting would need to be established from science-based transparent evidence, as the efficiency of CDR is very variable among regions. Mining sites should be optimally allocated to application areas for maximal CDR, maximal cost and emission efficiency, while taking the constraints on transport infrastructure into account. This would require substantial investment not only in transport and renewable energy infrastructure for the mining industry, but also in new technologies that would allow heavy cargo to be delivered to and spread over remote locations with a low-CO₂ footprint. Alternatively, ground-based deployment networks in combination with energy-efficient long-distance 'slurry pumps' as currently operated in the mining sector⁴⁸ could be used. Uncertain environmental risks and benefits associated with the release of trace elements in BD (for example, heavy metals and plant nutrients) for land, freshwater and coastal systems need to be considered. Besides the ongoing field trials in agricultural systems, the deployment in degraded forest and in afforestation/reforestation sites on impoverished or degraded soils should be tested to assess weathering and CDR efficiency and environmental issues. Regions where anthropogenic nitrogen deposits have promoted deficiencies in plant nutrition and soil acidification are of particular interest³⁹. Last, societal and political barriers^{3,7} need to be addressed. In particular, public engagement is needed to overcome the extremely low public awareness of this technology⁴⁹. An initial use of BD in agriculture, ecosystem restoration and afforestation may help to facilitate societal acceptance of more widespread application. If these barriers can be overcome, BD application in hinterlands could provide an important contribution to climate stabilization targets.

Online content

Any methods, additional references, Nature Research reporting summaries, source data, extended data, supplementary information, acknowledgements, peer review information; details of author contributions and competing interests; and statements of data and code availability are available at <https://doi.org/10.1038/s41561-021-00798-x>.

Received: 15 September 2020; Accepted: 16 June 2021;
Published online: 26 July 2021

References

- IPCC *Special Report on Global Warming of 1.5°C* (eds Masson-Delmotte, V. et al.) (WMO, 2018).
- Griscom, B. W. et al. Natural climate solutions. *Proc. Natl Acad. Sci. USA* **114**, 11645–11650 (2017).
- Smith, P. et al. Land-management options for greenhouse gas removal and their impacts on ecosystem services and the sustainable development goals. *Annu. Rev. Environ. Resour.* **44**, 255–286 (2019).
- Smith, P. et al. Biophysical and economic limits to negative CO₂ emissions. *Nat. Clim. Change* **6**, 42–50 (2016).
- Beerling, D. J. et al. Farming with crops and rocks to address global climate, food and soil security. *Nat. Plants* **4**, 138–147 (2018).
- Taylor, L. L. et al. Enhanced weathering strategies for stabilizing climate and averting ocean acidification. *Nat. Clim. Change* **6**, 402–406 (2016).
- Beerling, D. J. et al. Potential for large-scale CO₂ removal via enhanced rock weathering with croplands. *Nature* **583**, 242–248 (2020).
- Börker, J., Hartmann, J., Amann, T. & Romero-Mujalli, G. Terrestrial sediments of the Earth: development of a global unconsolidated sediments map database (gum). *Geochem. Geophys. Geosyst.* **19**, 997–1024 (2018).
- Dessert, C., Dupré, B., Gaillardet, J., François, L. M. & Allègre, C. J. Basalt weathering laws and the impact of basalt weathering on the global carbon cycle. *Chem. Geol.* **202**, 257–273 (2003).
- Dalmora, A. C. et al. Application of andesite rock as a clean source of fertilizer for eucalyptus crop: evidence of sustainability. *J. Clean. Prod.* **256**, 120432 (2020).
- Seifritz, W. CO₂ disposal by means of silicates. *Nature* **345**, 486 (1990).
- Köhler, P. Anthropogenic CO₂ of high emission scenario compensated after 3500 years of ocean alkalization with an annually constant dissolution of 5 Pg of olivine. *Front. Clim.* **2**, 575744 (2020).
- Peña-Ramírez, V. M., Vázquez-Solem, L. & Siebe, C. Soil organic carbon stocks and forest productivity in volcanic ash soils of different age (1835–30,500 years B.P.) in Mexico. *Geoderma* **149**, 224–234 (2009).
- de Oliveira Garcia, W. et al. Impacts of enhanced weathering on biomass production for negative emission technologies and soil hydrology. *Biogeosciences* **17**, 2107–2133 (2020).
- Kelland, M. E. et al. Increased yield and CO₂ sequestration potential with the C4 cereal *Sorghum bicolor* cultivated in basaltic rock dust-amended agricultural soil. *Glob. Chang. Biol.* **26**, 3658–3676 (2020).
- Ramos, C. G. et al. Evaluation of soil re-mineralizer from by-product of volcanic rock mining: experimental proof using black oats and maize crops. *Nat. Resour. Res.* **29**, 1583–1600 (2020).
- Tchouankoue, J., Tchekambou, A., Angue, M., Ngansop, C. & Theodoro, S. in *Geotherapy* (eds Goreau, T. J. et al.) 445–458 (CRC Press, 2014).
- Van Straaten, P. Farming with rocks and minerals: challenges and opportunities. *An. Acad. Bras. Cienc.* **78**, 731–747 (2006).
- Ramos, C. G. et al. Evaluation of the potential of volcanic rock waste from southern Brazil as a natural soil fertilizer. *J. Clean. Prod.* **142**, 2700–2706 (2017).
- Fuss, S. et al. Negative emissions - part 2: costs, potentials and side effects. *Environ. Res. Lett.* **13**, 2–4 (2018).
- Strefler, J., Amann, T., Bauer, N., Krieger, E. & Hartmann, J. Potential and costs of carbon dioxide removal by enhanced weathering of rocks. *Environ. Res. Lett.* **13**, 034010 (2018).
- de Oliveira Garcia, W., Amann, T. & Hartmann, J. Increasing biomass demand enlarges negative forest nutrient budget areas in wood export regions. *Sci. Rep.* **8**, 5280 (2018).
- Elser, J. J. et al. Global analysis of nitrogen and phosphorus limitation of primary producers in freshwater, marine and terrestrial ecosystems. *Ecol. Lett.* **10**, 1135–1142 (2007).
- Wright, S. J. Plant responses to nutrient addition experiments conducted in tropical forests. *Ecol. Monogr.* **89**, e01382 (2019).
- Hou, E. et al. Global meta-analysis shows pervasive phosphorus limitation of aboveground plant production in natural terrestrial ecosystems. *Nat. Commun.* **11**, 637 (2020).
- Du, E. et al. Global patterns of terrestrial nitrogen and phosphorus limitation. *Nat. Geosci.* **13**, 221–226 (2020).
- Terrer, C. et al. Nitrogen and phosphorus constrain the CO₂ fertilization of global plant biomass. *Nat. Clim. Change* **9**, 684–689 (2019).
- Gard, M. et al. Global whole-rock geochemical database compilation. *Earth Syst. Sci. Data* **11**, 1553–1566 (2019).
- Amann, T. & Hartmann, J. Ideas and perspectives: synergies from co-deployment of negative emission technologies. *Biogeosciences* **16**, 2949–2960 (2019).
- Cattaneo, A. et al. Global mapping of urban–rural catchment areas reveals unequal access to services. *Proc. Natl Acad. Sci. USA* <https://doi.org/10.1073/pnas.2011990118> (2021).
- Hartmann, J. et al. Enhanced chemical weathering as a geoengineering strategy to reduce atmospheric carbon dioxide, supply nutrients, and mitigate ocean acidification. *Rev. Geophys.* **51**, 113–149 (2013).
- Clair, T. & Hindar, A. Liming for the mitigation of acid rain effects in freshwater: a review of recent results. *Environ. Rev.* **13**, 91–128 (2005).
- Bošela, M. & Šebeň, V. Analysis of the aerial application of fertilizer and dolomitic limestone. *J. For. Sci.* **56**, 47–57 (2010).
- Grafton, M. C. E. et al. Resolving the agricultural crushed limestone flow problem from fixed wing aircraft. *Trans. ASABE* **54**, 769–775 (2011).
- Moosdorf, N., Renforth, P. & Hartmann, J. Carbon dioxide efficiency of terrestrial enhanced weathering. *Environ. Sci. Technol.* **48**, 4809–4816 (2014).
- IPCC *Special Report on Renewable Energy Sources and Climate Change Mitigation* (eds Edenhofer, O. et al.) (Cambridge Univ. Press, 2011).
- Cook, R. J., Barron, J. C., Papendick, R. I. & Williams, G. J. Impact on agriculture of the Mount St. Helens eruptions. *Science* **211**, 16–22 (1981).
- Doughty, C. E., Wolf, A. & Malhi, Y. The legacy of the Pleistocene megafauna extinctions on nutrient availability in Amazonia. *Nat. Geosci.* **6**, 761–764 (2013).
- Jonard, M. et al. Tree mineral nutrition is deteriorating in Europe. *Glob. Chang. Biol.* **21**, 418–430 (2015).

40. Peñuelas, J. et al. Human-induced nitrogen–phosphorus imbalances alter natural and managed ecosystems across the globe. *Nat. Commun.* **4**, 2934 (2013).
41. Wardle, D. A., Bardgett, R. D., Walker, L. R., Peltzer, D. A. & Lagerström, A. The response of plant diversity to ecosystem retrogression: evidence from contrasting long-term chronosequences. *Oikos* **117**, 93–103 (2008).
42. Kaspari, M. & Yanoviak, S. P. Biogeography of litter depth in tropical forests: evaluating the phosphorus growth rate hypothesis. *Funct. Ecol.* **22**, 919–923 (2008).
43. Harpole, W. S. et al. Addition of multiple limiting resources reduces grassland diversity. *Nature* **537**, 93–96 (2016).
44. Doughty, C. E., Abraham, A. & Roman, J. The sixth R: revitalizing the natural phosphorus pump. Preprint at *EcoEvoRxiv* <https://doi.org/10.32942/osf.io/45cnu> (2020).
45. *Status of the World's Soil Resources* (FAO & Intergovernmental Technical Panel on Soils, 2015).
46. Pai, S., Zerriffi, H., Jewell, J. & Pathak, J. Solar has greater techno-economic resource suitability than wind for replacing coal mining jobs. *Environ. Res. Lett.* **15**, 034065 (2020).
47. Korhonen, J., Honkasalo, A. & Seppälä, J. Circular economy: the concept and its limitations. *Ecol. Econ.* **143**, 37–46 (2018).
48. Macía, Y. M., Pedrera, J., Castro, M. T. & Vilalta, G. Analysis of energy sustainability in ore slurry pumping transport systems. *Sustainability* **11**, 3191 (2019).
49. Pidgeon, N. F. & Spence, E. Perceptions of enhanced weathering as a biological negative emissions option. *Biol. Lett.* **13**, 20170024 (2017).
50. Köhler, P. et al. Geoengineering potential of artificially enhanced silicate weathering of olivine. *Proc. Natl Acad. Sci. USA* **107**, 20228–20233 (2010).

Publisher's note Springer Nature remains neutral with regard to jurisdictional claims in published maps and institutional affiliations.

© Springer Nature Limited 2021

Methods

Modelling. We applied the global version (revision 5986, v1.2) of the nutrient-enabled land surface model ORCHIDEE-CNP (ref.⁵¹). The model simulates the exchange of GHGs (that is, CO₂ and nitrous oxide), water and energy at the land surface at a half-hourly time step, accounting for effects of nitrogen and P availability on plant productivity and organic matter decomposition. In the case of low nutrient availability, plant investment into root growth increases at the expense of leaf growth while foliar and fine root nutrient concentration is reduced, leading to lower plant productivity and carbon storage. Negative effects of nutrient shortages on plant productivity are partly compensated by higher activity of soil enzymes enhancing plant availability of P in soil organic matter and reduced losses of P by leaching due to the low P concentration in soil solution. The nutrient content of woody plant tissue is assumed to be rigid. More information is given in the Supplementary Note 1. The model is well evaluated at the site to global scale including nutrient leaching from terrestrial soils and the effects of elevated CO₂ on primary productivity and land carbon storage^{51–54}. The response of aboveground productivity to mineral P fertilizer addition compares well to observation-based estimates (Supplementary Note 1.3).

ORCHIDEE-CNP was coupled to a model for enhanced weathering that simulates the release of P and base cations from weathering of basalt grains in soils as a function of soil pH, soil temperature and basalt grain size, and basalt chemistry²¹. The abiotic CO₂ fixation pathway is based on the transfer of weathered base cations (that is, Ca²⁺, Mg²⁺, K⁺ and Na⁺) from soil drainage waters to surface waters that are charge balanced by the formation of bicarbonate (HCO₃⁻) ions and transported to the ocean, accounting for effects of ocean carbonate chemistry on CO₂ fixation. Owing to our focus on the role of the biotic CDR pathway, we omitted the role of ocean heterogeneity⁵⁵. The model was parameterized on dissolution reactions under controlled laboratory conditions. The scarce available data on basalt dissolution under field conditions indicate that rates are of the same order of magnitude as in the incubation experiments (Supplementary Note 2.2 and Supplementary Table 1). The P release during mineral dissolution is derived from the dissolution rate based on the P concentration of the grain assuming a homogeneous dissolution. A full description of the model can be found in Supplementary Note 2. Biological CDR is estimated by the differences in land carbon storage and nitrous oxide emissions between simulations with and without BD. Thereby we account for the background carbon sink due to legacy effects of historic changes in CO₂ concentration, climate and land use. BD can cause changes in nitrous oxide emissions due to plant-mediated BD effects on soil nitrogen and water, but the effects were found to be negligible in simulations (Supplementary Fig. 2). We assume a conversion factor of 298 to derive CO₂e from nitrous oxide emissions⁵⁶ to include them as part of CDR.

Model simulations were performed using reconstructed climate, atmospheric CO₂ concentration, land use and land management, and nitrogen and P inputs via atmospheric deposition, synthetic fertilizer and manure application. Information on soil conditions (soil pH, soil texture and bulk soil density) are prescribed from global reconstructions and are static in time. More details can be found in the Supplementary Note 1.1 and Supplementary Table 2. Starting from the year 2018, we ran 50-year simulations with different idealized scenarios of soil amendment with BD to all ice-free hinterland³⁰ excluding large deserts, as well as a baseline simulation without BD application (Supplementary Table 3). This does not represent a realistic deployment scenario, but is designed to give a first estimate of the full CDR potential of BD application in natural ecosystems and to identify regions with high CDR potential. We focus on hinterland ecosystems (that is, at a travel distance of more than 3 h from the nearest small city³⁰; Supplementary Fig. 1), to minimize potential interference with other land uses and human activities due to the increase in atmospheric particulate matter at the time of application or thereafter. The grain diameter of 20 µm was chosen such that the basalt applied to the hinterland area has mostly dissolved within five decades. Depending on the mode of deployment, larger particle sizes are preferable to reduce costs, energy demand of grinding, and environmental and health risks. The P content of basalt varies between geological formations^{28,29}. To account for this uncertainty, we conducted 3 × 3 simulations with either 1, 3 or 5 kg m⁻² of BD and three levels of P content: 0.161 ± 0.135 % weight (mean ± 1 standard deviation from ref.²⁸). We used repeated cycles of climate and deposition data for the period 2008–2017, keeping land cover and atmospheric CO₂ concentration fixed to their state in 2017. The initial state of the biogeochemical cycles is taken from ref.³⁰ and accounts for historical changes in atmospheric CO₂ concentration, atmospheric nutrient deposition, land cover and land management (mineral fertilizer and manure) since 1700. We use a grain size of 20 µm, which is cost efficient in the production process²¹ and penetrates into deeper soil layers through water percolation and bioturbation³⁶. For P content we prescribe average ± standard deviation P of basalt from *n* = 65,363 samples in the GEOROC database²⁸.

Cost analysis. Cost assessment is needed to evaluate commercial feasibility of BD and to put a price on climate mitigation actions. The main economic costs for BD are mining, crushing and grinding of rocks, and transport to and distribution over target areas. Here we assume application with helicopters or small fixed-wing aircraft equipped with agricultural spreaders that can carry up to 4 t over a range of ~1,000 km (refs. 32–34). Dust is either mixed with water in a ratio of 1:5 (ref.³⁵)

or used as free-flowing particles (size > 500 µm)³³. We calculate the costs based on present-day costs compiled by refs. 7,50,21. These estimated costs account for uncertainties with respect to energy costs, airborne application and variation between open-pit mines. Here we briefly summarize the approach—details are listed elsewhere²¹. Costs for mining, crushing and grinding (*c_{mine}*) consist of specific investment costs (*c_{inv}*), operation and maintenance costs (*c_{OM}*) and energy costs (*c_m*): *c_{mine}* = *c_{inv}* + *c_{OM}* + *c_m*. The associated costs (range) were extracted from economic assessment reports for open-pit mines: *c_{inv}* = US\$5.0 (2.2–8.5) t⁻¹, *c_{OM}* = US\$25.1 (15.2–33.5) t⁻¹. The electricity demand for mining and crushing ranges between 0.01 and 0.03 GJ t⁻¹, and for grinding ranges between 0.069 and 0.6095 GJ t⁻¹ for the target grain size of 20 µm. Electricity prices can vary substantially by region and over time. As a first-order cost estimate, we take the median electricity prices among the EU15 and G7 states (US\$27.5 GJ⁻¹) for the year 2018⁷. Costs for ground transportation from mines to airfields (*c_{tran}* = US\$8.57–9.21 t⁻¹) and spreading the ground rock by small aircraft (*c_{air}* = US\$88–171 t⁻¹) are a function of mass and consist of fuel costs and specific costs (for example, for labour) and were taken from ref.⁵⁰: *c_{app}* = *c_{tran}* + *c_{air}*. Total costs are given by the sum of *c_{mine}* and *c_{app}*: US\$174 (116–239) t⁻¹.

GHG emissions from BD. The main GHG emissions are related to the mining, crushing and grinding of rocks, and transport to and distribution on target areas; these depend strongly on the energy production system^{7,19} and transport systems. We collected information on GHG emissions (gCO₂e kWh⁻¹) based on a literature review of life cycle analysis of electricity generation technologies (gCO₂e kWh⁻¹; ref.⁵⁷) and transport systems (tCO₂e per tonne of rock per kilometre)⁵⁸ for the present day (Supplementary Table 8). The GHG emission can be calculated by combining the energy requirement of mining and grinding of rock material (see above) with the transport distance. The transport distance was approximated by the shortest distance between the nearest location of basalt reserves mineable with current technology⁸ and the respective model pixel. Extended Data Fig. 3 shows the GHG emissions as a function of transport distance for different combinations of transport and energy production systems.

Global mining capacity. The global capacity was approximated using the data for the top five most-mined minerals, namely: coal, iron, bauxite, phosphate and gypsum. A total of 11.78 Gt of rock was mined in the year 2017⁵⁹. Coal mining is the dominant sector by far (Supplementary Table 9).

Data availability

The simulation data (<https://doi.org/10.5281/zenodo.3963784>, <https://doi.org/10.14768/20200407002.1>) are freely available. The dataset on airfield location is available at <https://openflights.org/data.html> (accessed 18 January 2020).

Code availability

The source code of the land surface model ORCHIDEE-CNP is freely available (<https://doi.org/10.14768/20200407002.1>). The corresponding author will make the Python codes developed for this study available upon reasonable request.

References

- Goll, D. S. et al. A representation of the phosphorus cycle for ORCHIDEE (revision 4520). *Geosci. Model Dev.* **10**, 20228–20233 (2017).
- Goll, D. S. et al. Low phosphorus availability decreases susceptibility of tropical primary productivity to droughts. *Geophys. Res. Lett.* **45**, 8231–8240 (2018).
- Sun, Y. et al. Global evaluation of the nutrient-enabled version of the land surface model ORCHIDEE-CNP v1.2 (r5986). *Geosci. Model Dev.* **14**, 1987–2010 (2021).
- Friedlingstein, P. et al. Global carbon budget. *Earth Syst. Sci. Data* **11**, 1783–1838 (2019).
- Ilyina, T. et al. Assessing the potential of calcium-based artificial ocean alkalization to mitigate rising atmospheric CO₂ and ocean acidification. *Geophys. Res. Lett.* **40**, 5909–5914 (2013).
- Fishkis, O., Ingwersen, J., Lamers, M., Denysenko, D. & Streck, T. Phytolith transport in soil: a field study using fluorescent labelling. *Geoderma* **157**, 27–36 (2010).
- Artaxo, P. et al. in *Climate Change 2007: The Physical Science Basis* (eds Solomon, S. et al.) Ch. 2 (IPCC, Cambridge Univ. Press, 2007).
- Guidelines for Measuring and Managing CO₂ Emission from Freight Transport Operations* (ECTA, March 2011).
- Brown, T. J. et al. *World Mineral Production 2013–17* (British Geological Survey, 2019).

Acknowledgements

D.S.G., P.C., J.P., M.O., I.J. and S.V. acknowledge financial support from the European Research Council Synergy grant ERC-SyG-2013-610028 IMBALANCE-P. J.P. acknowledges financial support from the Spanish Government grant

PID2019-110521GB-I00, the Fundación Areces grant ELEMENTAL-CLIMATE and the Catalan Government grant SGR 2017-1005. D.S.G. and P.C. benefited from support from the Agence Nationale de la Recherche (ANR) grant ANR-16-CONV-0003 (CLAND). T.A. and J.H. benefited from financial support from the Deutsche Forschungsgemeinschaft (DFG, German Research Foundation) priority programme on 'Climate Engineering-Risks, Challenges and Opportunities?', specifically the CEMICS2 project, and under Germany's Excellence Strategy – EXC 2037 'Climate, Climatic Change, and Society' – project number 390683824, contribution to the Center for Earth System Research and Sustainability (CEN) of Universität Hamburg. K.T. benefited from State assistance managed by the National Research Agency in France under the 'Programme d'Investissements d'Avenir' under the reference ANR-19-MPGA-0008.

Author contributions

D.S.G., P.C. and T.A. designed the study. D.S.G. and J.C. undertook model development and coding, with input from W.L. and T.A. T.A. provided data on rock chemistry. D.S.G. undertook the data analysis and synthesis. D.S.G. wrote the manuscript with

input on sections and addition of appropriate references specific to their area of expertise from all authors.

Competing interests

The authors declare no competing interests.

Additional information

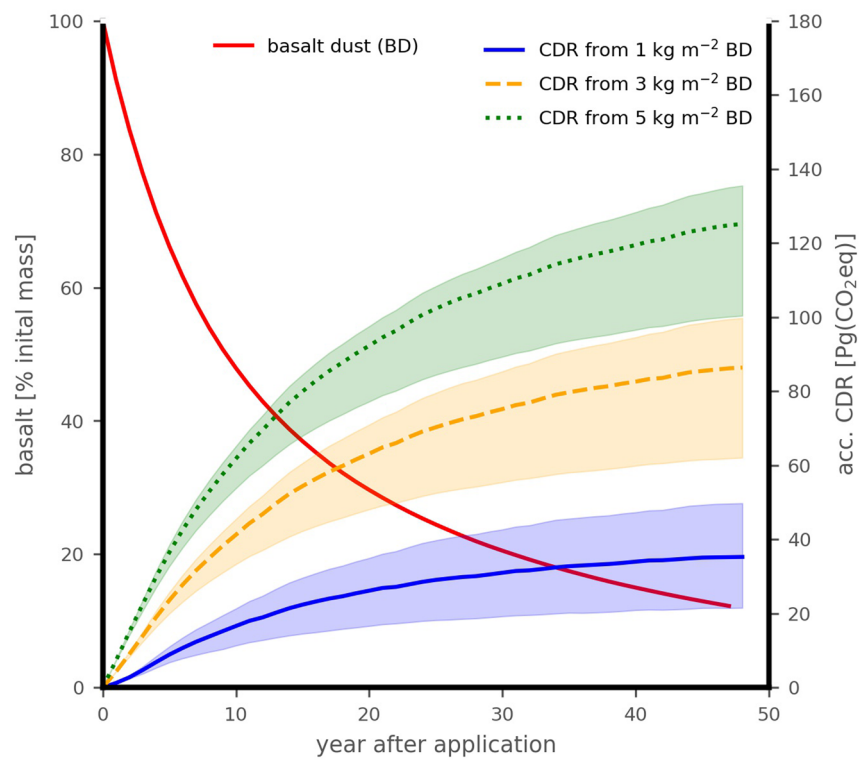
Extended data is available for this paper at <https://doi.org/10.1038/s41561-021-00798-x>.

Supplementary information The online version contains supplementary material available at <https://doi.org/10.1038/s41561-021-00798-x>.

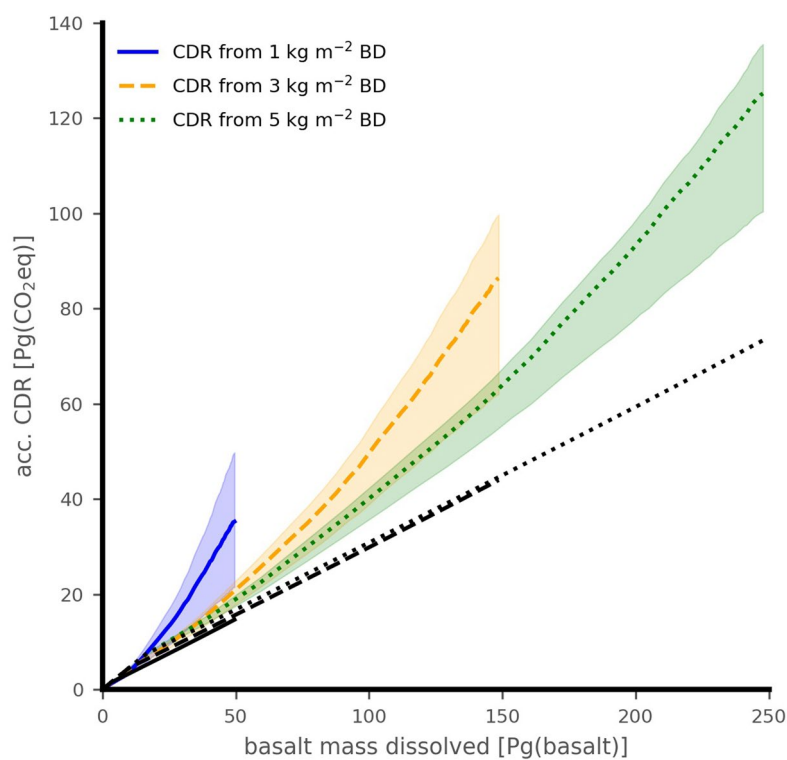
Correspondence should be addressed to D.S.G.

Peer review information *Nature Geoscience* thanks the anonymous reviewers for their contribution to the peer review of this work. Primary Handling Editor: Xujia Jiang.

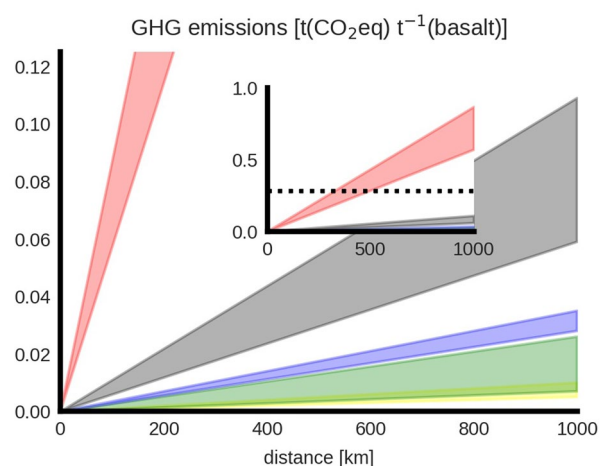
Reprints and permissions information is available at www.nature.com/reprints.



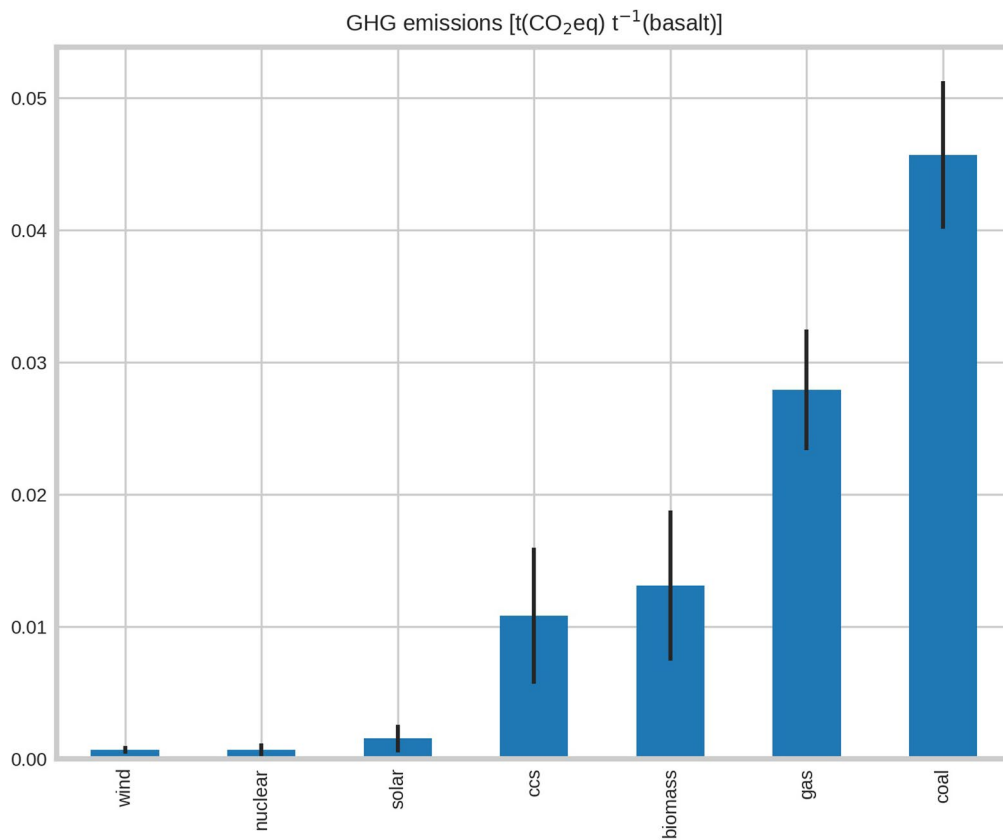
Extended Data Fig. 1 | Carbon dioxide removal (CDR) and dissolution of basalt dust (BD) over the course of the experiment. The accumulated CDR is given for one-time basalt dust additions of 1, 3 and 5 kg m⁻² and varying P contents ranging between 0.036 and 0.286 %-weight (shaded areas). Remaining BD mass is shown in red.



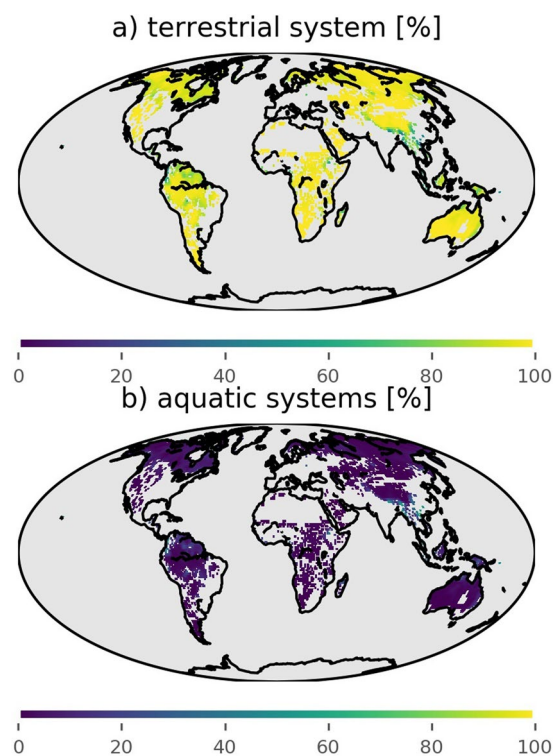
Extended Data Fig. 2 | The trajectories of carbon dioxide removed (CDR) as a function of the amount of dissolved basalt dust. Shown is CDR for different amounts of basalt dust addition of 1, 3, and 5 kg m⁻² (color) and varying P contents ranging between 0.036 and 0.286 %-weight (shaded areas). Abiotic CDR is shown in black.



Extended Data Fig. 3 | Greenhouse gas (GHG) emissions from the distribution of basalt dust. Shown are emissions for a selection of existing transport technologies (airplane [red], road [grey], railroad [green], river [blue] & pipeline [yellow]) as a function of transportation distance. The shaded areas represent the variation in GHG emission within a transport type. The dotted line shows the median CDR potential of basalt application to hinterlands.

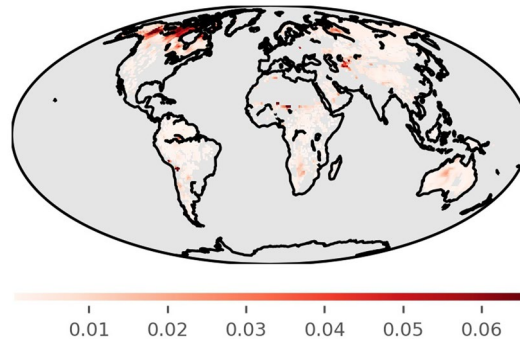


Extended Data Fig. 4 | Greenhouse gas (GHG) emissions from the production of basalt dust. Shown are median GHG emissions for selected energy production systems: wind, nuclear, concentrated solar power, coal power coupled to carbon capture and storage (ccs), biomass burning (dedicated), gas (combined cycle), and coal (pulverized). The bars indicate maximum and minimum values.



Extended Data Fig. 5 | The fate of basalt derived phosphorus. Shown are the fractions of phosphorus released from basalt dust which remains in terrestrial ecosystems (top) or is lost to aquatic systems (bottom) 50 years after application of 5 kg m^{-2} basalt dust of intermediate P content (0.161 %-weight).

Change in runoff P concentration [$\mu\text{g/L}$]



Extended Data Fig. 6 | Increase in phosphorus concentration in surface runoff due to basalt dust application. Shown is the increase in phosphorus concentration averaged for the 50 years after application of 5 kg m^{-2} basalt dust of intermediate P content (0.161 %-weight).